VIP Electrocatalysis Very Important Paper

International Edition: DOI: 10.1002/anie.201702578
German Edition: DOI: 10.1002/ange.201702578

A Membrane-Free Neutral pH Formate Fuel Cell Enabled by a Selective Nickel Sulfide Oxygen Reduction Catalyst

*Bing Yan, Nolan M. Concannon, Jarrod D. Milshtein, Fikile R. Brushett, and Yogesh Surendranath**

Abstract: *Polymer electrolyte membranes employed in contemporary fuel cells severely limit device design and restrict catalyst choice, but are essential for preventing short-circuiting reactions at unselective anode and cathode catalysts. Herein, we report that nickel sulfide Ni_3S_2 is a highly selective catalyst for the oxygen reduction reaction in the presence of 1.0 M formate. We combine this selective cathode with a carbon-supported palladium (Pd/C) anode to establish a membrane-free, room-temperature formate fuel cell that operates under benign neutral pH conditions. Proof-of-concept cells display open circuit voltages of approximately 0.7 V and peak power values greater than 1 mW cm^{-2}, significantly outperforming the identical device employing an unselective platinum (Pt) cathode. The work establishes the power of selective catalysis to enable versatile membrane-free fuel cells.*

Fuel cells enable the conversion of chemical energy into electrical energy with efficiencies that can exceed the Carnot limit.[1,2] Central to the operation of all commercial fuel cells is an ion-selective membrane that serves to separate the anode and cathode reactions while permitting the transport of charge-balancing electrolyte ions.[3–5] Importantly, this membrane must impede the cross-over of fuel and oxidant between the anode and cathode to prevent short-circuiting reactions that degrade the power output of the fuel cell. The physical properties of the membrane, in most cases, dictate the range of viable anode and cathode catalysts. For example, Nafion and its derivatives, which are widely used in commercial polymer-electrolyte membrane fuel cells (PEMFCs), consist of highly acidic sulfonic acid groups, limiting the range of viable catalysts employed in PEMFCs to those that resist acid-mediated corrosion. While a far wider range of materials are stable at intermediate or alkaline environments, membranes that are operative under these conditions[6,7] suffer from either poor proton/hydroxide conductivity or limited stability,[8–10] curtailing the development of intermediate or alkaline pH PEMFC devices.

In principle, the membrane could be eliminated altogether, if selective catalysts for the anode and cathode reactions can be developed. Membrane-free fuel cells are particularly attractive for carbonaceous fuels, such as methanol and formic acid, which form stable mixtures with O_2. Additionally, membrane-free configurations can afford a greater degree of flexibility in electrode arrangement, electrolyte choice, and device design, all of which lower the cost of cell-construction.[11,12] Achieving high performance in a membrane-free configuration requires that the cathode selectively reduces O_2 (Figure 1a, black) without oxidizing the fuel (Figure 1a, red) and that the anode selectively oxidizes the fuel (Figure 1a, black) without reducing O_2 (Figure 1a, red).[11] This selectivity is particularly challenging because the driving force for the undesirable short-circuiting reactions—fuel oxidation at the cathode and oxygen reduction at the anode (Figure 1b, red)—are significantly greater than the driving force for the desired reactions (Figure 1b, black) at each electrode.[13] This problem is magnified at the cathode, in particular, because the dissolved O_2 concentration (<1 mM) is typically far lower than the concentration of the liquid fuel. While these stringent selectivity requirements can be met by several enzymatic or microbial catalysts,[14–16] biological fuel cells suffer from limited power densities,[17–19] motivating the development of abiotic alternatives. However, there exist a paucity of examples[11–15] of abiotic membrane-free fuel cells, and all prior reports operate in alkaline environments where long-term operation of a carbonaceous

[*] B. Yan, N. M. Concannon, Prof. Dr. Y. Surendranath
Department of Chemistry
Massachusetts Institute of Technology
77 Massachusetts Ave., Cambridge, MA 02139-4307 (USA)
E-mail: yogi@mit.edu
J. D. Milshtein
Department of Materials Science and Engineering
Massachusetts Institute of Technology
77 Massachusetts Ave., Cambridge, MA 02139-4307 (USA)
Prof. Dr. F. R. Brushett
Department of Chemical Engineering
Massachusetts Institute of Technology
77 Massachusetts Ave., Cambridge, MA 02139-4307 (USA)
Supporting information and the ORCID identification number(s) for the author(s) of this article can be found under: https://doi.org/10.1002/anie.201702578.

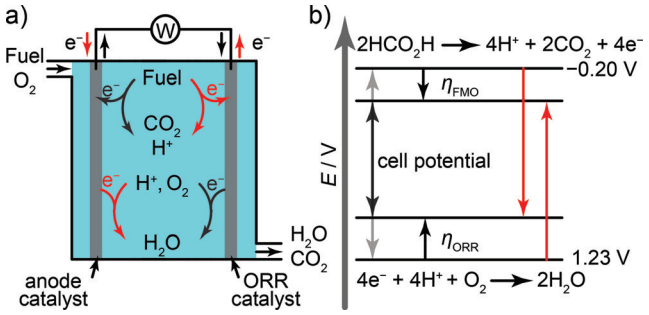

Figure 1. a) Schematic of a membrane-free carbonaceous fuel cell depicting the desirable fuel combustion (black) and undesirable parasitic short-circuit reactions (red). b) Energy diagram of the fuel cell depicting the driving forces for the desirable fuel combustion reactions (black arrows) and the undesirable parasitic reactions (red arrows).

fuel cell is prohibited by the absorption of CO_2 into the electrolyte, thereby decreasing the pH.[6,23,24] Thus, the construction of a viable carbonaceous fuel cell requires the development of selective catalysts[25] that operate near the buffering point (pH ca. 7) of the bicarbonate/CO_2 pair such that the CO_2 produced at the anode is released from the solution.

Recently, we reported that Ni_3S_2 is a potent catalyst for the oxygen reduction reaction (ORR) at neutral pH conditions and is remarkably tolerant to buffering electrolytes such as phosphate.[26] Herein, we show that this material is also highly selective for the ORR even in the presence of 1.0 M potassium formate (HCO_2K), and we pair this selective ORR catalyst with a known formate/formic acid oxidation catalyst, Pd/C,[27–30] to develop an abiotic, membrane-free, neutral pH fuel cell for the first time.

To isolate the intrinsic selectivity and activity of Ni_3S_2 and Pd in the absence of convoluting solution resistance or transport limitations, we performed three-electrode measurements on a rotating disk electrode (RDE). Ni_3S_2 (see Figure S1 in the Supporting Information) was prepared by high temperature solid state synthesis: stoichiometric nickel and sulfur powder were mixed thoroughly in a mortar and pestle, and heated at 600 °C for 24 h followed by heating at 800 °C for another 4 h. Commercial Pd/C was used as received as the anode catalyst. Catalyst-coated electrodes were prepared by drop casting a catalyst-Nafion suspension in ethanol onto glassy carbon RDEs. Consistent with our previous observations,[26] in O_2-saturated 0.1 M potassium phosphate (KP_i), pH 7, linear sweep voltammograms (LSV) (Figure 2a, black) reveal that Ni_3S_2 catalyzes the ORR with an onset potential (defined as the potential corresponding to a current density of $-0.10\ mA\,cm^{-2}$) of 0.77 V (all potentials are reported versus the reversible hydrogen electrode (RHE)). Remarkably, a very similar voltammetric profile (Figure 2a, red) is observed in 0.1 M KP_i electrolyte containing 1.0 M HCO_2K. We observe a small negative shift in the ORR onset potential to 0.75 V and a slight diminishment (ca. 11%) in the magnitude of the catalytic current at 0.4 V. Importantly, these small changes in ORR activity can be entirely ascribed to the 20–30% decrease in O_2 solubility in water upon increasing the ionic strength from 0.1 to 1.1 M.[31,32] Indeed, we observe a comparable decrease in ORR current at 0.4 V for Ni_3S_2/C in O_2-saturated 1.0 M KP_i compared to 0.1 M KP_i (Figure S2). Together, the data evinces the excellent selectivity of Ni_3S_2 for the ORR even in the presence of a vast excess of the formate fuel.

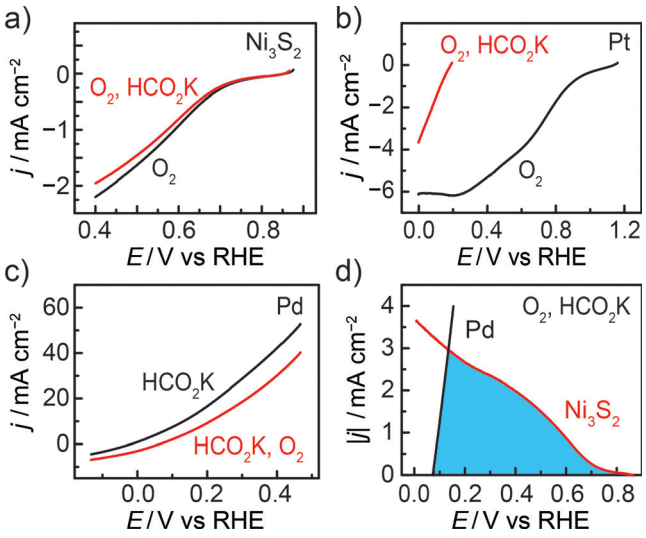

Figure 2. The LSV of a) Ni_3S_2/C and b) Pt/C recorded in O_2-saturated 0.1 M KP_i, pH 7, electrolyte with (red) and without (black) 1.0 M HCO_2K. c) LSV of Pd/C in N_2- (black) and O_2-saturated (red) 0.1 M KP_i, pH 7, electrolyte containing 1.0 M HCO_2K. d) Overlay of LSV curves recorded in O_2-saturated (red) 0.1 M KP_i, pH 7, electrolyte containing 1.0 M HCO_2K, with the absolute values of the current density for Ni_3S_2/C (red) and Pd/C (black). All data were collected at 5 $mV\,s^{-1}$ scan rate and 2000 rpm rotation rate.

In contrast, Pt, the most active known ORR catalyst, is entirely unselective for the ORR in the presence of the formate fuel. In the absence of the fuel, the Pt electrode displays an open circuit potential (OCP) of 1.14 V (Figure 2b, black) in O_2-saturated 0.1 M KP_i, pH 7, electrolyte, consistent with its high activity for the ORR. However, in the presence of 1.0 M HCO_2K, the OCP shifts negatively (Figure 2b, red) by nearly 1.0 V to 0.18 V. Additionally, in the presence of the fuel, a large anodic current attributed to formate oxidation is observed at potentials positive of approximately 0.2 V (Figure S3). Together, these results indicate that in striking contrast to Ni_3S_2, Pt is unselective for the ORR and that the undesirable fuel oxidation dominates in the presence of formate.

Unlike Ni_3S_2, the Pd/C anode catalyzes both formate oxidation and the ORR in O_2-saturated formate-containing electrolyte. LSV data recorded in O_2-saturated 0.1 M KP_i electrolyte, containing 1.0 M HCO_2K, (Figure 2c, red) reveals appreciable cathodic current between 0 V and 0.1 V that is not observed in the N_2-saturated electrolyte (Figure 2c, black). The data indicate that the cathodic ORR dominates the aggregate current response at low potentials, but, as the driving force for fuel oxidation increases with polarization to more positive values, the anodic fuel oxidation current exceeds the parasitic ORR current, leading to a net anodic current flow. We note that, unlike the Ni_3S_2 cathode, which selectively catalyzes the ORR in the presence of the fuel, the Pd/C anode catalyzes the desirable fuel oxidation reaction as well as the short-circuiting ORR. Indeed, the Pd/C anode generates net anodic current principally as a result of the high concentration of the 1.0 M HCO_2K fuel relative to the <1 mM concentration of dissolved O_2 in the electrolyte.[31] Nevertheless, the poor selectivity of Pd/C anode is the principal impediment to fuel cell efficiency, and selective inorganic catalysts for fuel oxidation are, to the best of our knowledge, non-existent. Thus, these data motivate the development of O_2-tolerant anode catalysts to enable high performance membrane-free fuel cells.[33]

The foregoing three-electrode studies on RDEs examined the catalytic activity and selectivity of each electrode in the absence of appreciable resistive or transport losses, allowing us to estimate the theoretical performance of a combined device. An overlay of the LSV curves with the absolute values of the current density of the Ni_3S_2 cathode and the Pd/C anode recorded in O_2-saturated 0.1 M KP_i, 1.0 M HCO_2K

electrolyte is shown in Figure 2d. At zero current, the potential gap between the two LSV curves is 0.77 V, correlating to the expected open circuit voltage (OCV) of a Ni_3S_2-Pd fuel cell. As the current increases, the potential difference decreases, indicating that the output power (the shaded area in Figure 2d), $P = (j \times E)$, of the device will reach a peak value at an intermediate cell voltage.

Data from the three-electrode studies were used to optimize the formate fuel concentration of the membrane-free fuel cell. LSV curves reveal that while higher formate concentrations increase the current going towards fuel oxidation at the anode, at a very high fuel concentration, 2.0 M HCO_2K, we observed a pronounced suppression in ORR current at the Ni_3S_2 cathode that we attribute to a dramatic reduction in O_2 solubility in the electrolyte (Figure S4, red). On the other hand, at a low formate concentration, 0.2 M HCO_2K, O_2 reduction dominates the current response at the Pd/C anode relative to the desirable fuel oxidation reaction (Figure S4, blue). This undesirable performance is also reflected in simulated power curves calculated from the LSV data (Figure S5). Given these observations, we selected an intermediate fuel concentration of 1.0 M HCO_2K to balance the competing effects of anode selectivity and O_2 solubility.

To validate the feasiblity of a neutral pH membrane-free fuel cell, we constructed a flow-through two-electrode proof-of-concept device (Figure 3). The cell was constructed using a simple 0.64 cm Teflon Swagelok union. 80 μL of Ni_3S_2/C and Pd/C suspensions were drop cast onto 0.48 cm-diameter, 0.32 cm-thick carbon felt electrodes, which serve as the cathode and anode, respectively (see SI for details of cell fabrication). Instead of a conventional ion-selective membrane, this membrane-free architecture simply employed polypropylene/cellulose paper separators sandwiched by 0.48 cm-diameter carbon paper to maximize electrical contact to the catalyst, and prevent adventitious transfer of catalyst particles from one electrode to the other. Electrical contact to the cathode and anode was furnished by graphite tube current collectors, and O_2-saturated electrolyte containing the formate fuel was flowed at a constant rate through the assembly from the cathode to the anode. This simple device architecture is effective for generating power from the formate/O_2 mixture at room temperature. At a flow rate of 0.1 mL min^{-1} we observe an OCV of approximately 0.7 V and a peak power density of 1.6 mW cm^{-2} (Figure 4a, black). The peak power density of this proof-of-concept cell is approximately one order of magnitude greater than typical microbial formate fuel cells operating under similar conditions,[34–38] evincing the potential of selective inorganic catalysis to enable high performance membrane-free technologies.

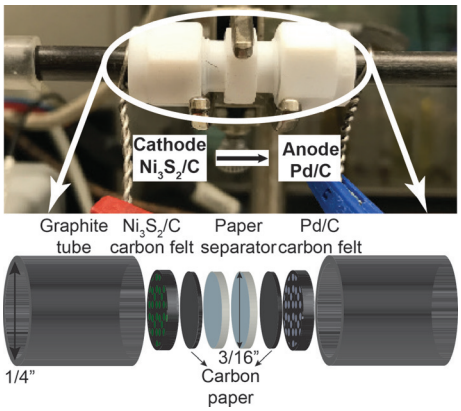

Figure 3. Schematic diagram of a flow-through, two-port membrane-free formate fuel cell. Inside the cell: graphite tube current collectors, carbon felt electrodes, carbon paper and separator. The O_2-saturated 0.1 M KP_i, 1.0 M HCO_2K electrolyte is flowed from the cathode to the anode.

As highlighted above, the Pd/C anode displays poor selectivity for fuel oxidation (Figure 2c), and this factor is reflected in the operation of the combined device. In particular, reversing the flow direction such that the fuel/O_2 mixture contacts the anode prior to the cathode (Figure 4a, red) leads to a four-fold drop in peak power from 1.6 to 0.4 mW cm^{-2}, consistent with significant O_2 consumption at the Pd/C anode, effectively depleting the oxidant concentration experienced by the cathode and lowering the peak power. The same trend is observed at higher flow rates (Figure S6), but the difference in performance upon changing the direction of flow is diminished at elevated flow rate due to the higher overall flux of O_2 to the cell. Together, these observations motivate the development of highly selective fuel oxidation catalysts to enable higher performance membrane-free fuel cells.

Owing to the excellent selectivity of Ni_3S_2 for ORR in the presence of the fuel, the Ni_3S_2-Pd fuel cell displays superior performance to a Pt-Pd setup under identical operating

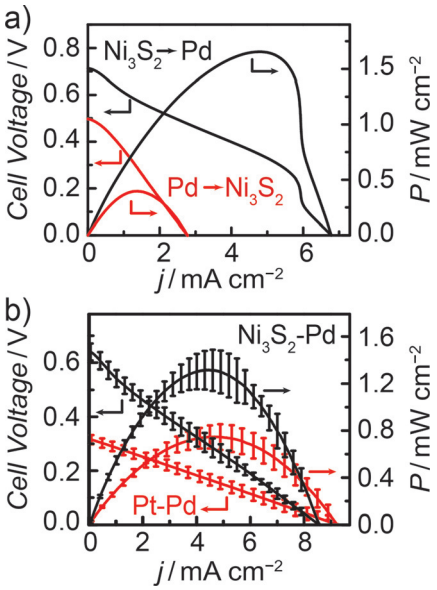

Figure 4. a) Cell voltage (left axis) and power density (right axis) versus current density plots for a Ni_3S_2-Pd membrane-free fuel cell operated with O_2-saturated 0.1 M KP_i, 1.0 M HCO_2K, pH 7, electrolyte flowed at 0.1 mL min^{-1} from the cathode (Ni_3S_2/C) to the anode (Pd/C) (black) and from the anode to the cathode (red). b) Cell voltage (left axis) and power density (right axis) versus current density plots for Ni_3S_2-Pd (black) and Pt-Pd (red) membrane-free fuel cells operated with O_2-saturated 0.1 M KP_i, 1.0 M HCO_2K, pH 7, electrolyte flowed at 1.0 mL min^{-1} from the cathode to the anode. Data are the average and standard error of five independently assembled fuel cells.

conditions. While Ni_3S_2-Pd fuel cells display average peak power densities of (1.3 ± 0.2) mW cm^{-2} and OCVs of (0.64 ± 0.01) V at a 1.0 mL min^{-1} flow rate (Figure 4b, black), Pt-Pd fuel cells only achieve average peak power densities of (0.7 ± 0.1) mW cm^{-2} and OCVs of (0.32 ± 0.01) V (Figure 4b, red). These data further establish that catalyst selectivity is a key determinant of the cell performance in a membrane-free device.

We have developed a proof-of-concept abiotic membrane-free formate fuel cell that operates under benign conditions: neutral pH, room temperature, 1 atm. The device combines a highly selective Ni_3S_2/C cathode with a Pd/C anode to effectively generate power from a mixed formate/O_2 stream. Owing to the high selectivity of Ni_3S_2 for the ORR in the presence of the fuel, this system significantly outperforms an analogous Pt-Pd device under identical conditions. The benign conditions of operation make the Ni_3S_2 cathode and this device configuration ideal for coupling with enzymatic or microbial anodes, thereby enabling the oxidation of more complex fuels such as glucose and acetate.[39–41] This work establishes the power of selective catalysis in enabling membrane-free fuel cells for versatile portable power applications.

Acknowledgements

We gratefully acknowledge Anna Wuttig, Youngmin Yoon, R. Soyoung Kim, Dr. Christopher Hendon, Dr. Matthew O'Reilly and Dr. Sahr Khan for helpful discussions. This research was supported by the NSF under award CHE-1454060, and by the MIT Department of Chemistry through junior faculty funds for Y.S. This work made use of the MRSEC Shared Experimental Facilities at MIT, which is supported in part by the NSF under award DMR-0819762.

Conflict of interest

The authors declare no conflict of interest.

Keywords: electrocatalysis · formate · fuel cells · heterogeneous catalysis · oxygen reduction

How to cite: *Angew. Chem. Int. Ed.* **2017**, *56*, 7496–7499
Angew. Chem. **2017**, *129*, 7604–7607

[1] L. Carrette, K. A. Friedrich, U. Stimming, *Fuel Cells* **2001**, *1*, 5–39.
[2] M. Winter, R. J. Brodd, *Chem. Rev.* **2004**, *104*, 4245–4269.
[3] P. L. Hentall, J. B. Lakeman, G. O. Mepsted, P. L. Adcock, J. M. Moore, *J. Power Sources* **1999**, *80*, 235–241.
[4] N. Sammes, F. Barbir, *Fuel Cell Technology,* Springer-Verlag, London, **2006**, 27–51.
[5] V. Mehta, J. S. Cooper, *J. Power Sources* **2003**, *114*, 32–53.
[6] J. R. Varcoe, R. C. T. Slade, *Fuel Cells* **2005**, *5*, 187–200.
[7] G. Merle, M. Wessling, K. Nijmeijer, *J. Membr. Sci.* **2011**, *377*, 1–35.
[8] A. A. Zagorodni, D. L. Kotova, V. F. Selemenev, *React. Funct. Polym.* **2002**, *53*, 157–171.
[9] V. Neagu, I. Bunia, *Polym. Degrad. Stab.* **2004**, *83*, 133–138.
[10] V. Neagu, I. Bunia, I. Plesca, *Polym. Degrad. Stab.* **2000**, *70*, 463–468.
[11] M. A. Priestnall, V. P. Kotzeva, D. J. Fish, E. M. Nilsson, *J. Power Sources* **2002**, *106*, 21–30.
[12] M. Nagao, M. Takahashi, T. Hibino, *Energy Environ. Sci.* **2010**, *3*, 1934–1940.
[13] J. G. Speight, *Lange's Handbook of Chemistry*, McGRAW-HILL, Laramie, WY, **2005**, 1.382.
[14] B. Friedrich, J. Fritsch, O. Lenz, *Curr. Opin. Biotechnol.* **2011**, *22*, 358–364.
[15] J. Fritsch, P. Scheerer, S. Frielingsdorf, S. Kroschinsky, B. Friedrich, O. Lenz, C. M. T. Spahn, *Nature* **2011**, *479*, 249–252.
[16] T. Burgdorf, O. Lenz, T. Buhrke, E. van der Linden, A. K. Jones, S. P. J. Albracht, B. Friedrich, *J. Mol. Microbiol. Biotechnol.* **2005**, *10*, 181–196.
[17] Z. Du, H. Li, T. Gu, *Biotechnol. Adv.* **2007**, *25*, 464–482.
[18] D. Pant, G. Van Bogaert, L. Diels, K. Vanbroekhoven, *Bioresour. Technol.* **2010**, *101*, 1533–1543.
[19] J. R. Trapero, L. Horcajada, J. J. Linares, J. Lobato, *Appl. Energy* **2017**, *185*, 698–707.
[20] A. Aziznia, C. W. Oloman, E. L. Gyenge, *J. Power Sources* **2014**, *265*, 201–213.
[21] X. Yu, A. Manthiram, *Appl. Catal. B* **2015**, *165*, 63–67.
[22] S. C. Barton, T. Patterson, E. Wang, T. Fuller, A. West, *J. Power Sources* **2001**, *96*, 329–336.
[23] P. Gouérec, L. Poletto, J. Denizot, E. Sanchez-Cortezon, J. H. Miners, *J. Power Sources* **2004**, *129*, 193–204.
[24] G. F. McLean, T. Niet, S. Prince-Richard, N. Djilali, *Int. J. Hydrogen Energy* **2002**, *27*, 507–526.
[25] L. Hussein, Y. J. Feng, N. Alonso-Vante, G. Urban, M. Krüger, *Electrochim. Acta* **2011**, *56*, 7659–7665.
[26] J. M. Falkowski, N. M. Concannon, B. Yan, Y. Surendranath, *J. Am. Chem. Soc.* **2015**, *137*, 7978–7981.
[27] A. Chen, C. Ostrom, *Chem. Rev.* **2015**, *115*, 11999–12044.
[28] K. Jiang, H.-X. Zhang, S. Zou, W.-B. Cai, *Phys. Chem. Chem. Phys.* **2014**, *16*, 20360–20376.
[29] S.-I. Choi, J. A. Herron, J. Scaranto, H. Huang, Y. Wang, X. Xia, T. Lv, J. Park, H.-C. Peng, M. Mavrikakis, et al., *ChemCatChem* **2015**, *7*, 2077–2084.
[30] H. Jeon, B. Jeong, M. Choun, J. Lee, *Electrochim. Acta* **2014**, *140*, 525–528.
[31] E. Narita, F. Lawson, K. N. Han, *Hydrometallurgy* **1983**, *10*, 21–37.
[32] A. Schumpe, I. Adler, W.-D. Deckwer, *Biotechnol. Bioeng.* **1978**, *20*, 145–150.
[33] R. Kamai, K. Kamiya, K. Hashimoto, S. Nakanishi, *Angew. Chem. Int. Ed.* **2016**, *55*, 13184–13188; *Angew. Chem.* **2016**, *128*, 13378–13382.
[34] X. Quan, B. Sun, H. Xu, *Electrochim. Acta* **2015**, *182*, 815–820.
[35] Y. Ojima, T. Kawata, N. Matsuo, Y. Nishinoue, M. Taya, *Bioprocess Biosyst. Eng.* **2014**, *37*, 2005–2008.
[36] M. Rosenbaum, U. Schröder, F. Scholz, *J. Solid State Electrochem.* **2006**, *10*, 872–878.
[37] P. T. Ha, B. Tae, I. S. Chang, *Energy Fuels* **2008**, *22*, 164–168.
[38] J. Kan, L. Hsu, A. C. M. Cheung, M. Pirbazari, K. H. Nealson, *Environ. Sci. Technol.* **2011**, *45*, 1139–1146.
[39] H. Yuan, Y. Hou, I. M. Abu-Reesh, J. Chen, Z. He, *Mater. Horiz.* **2016**, *3*, 382–401.
[40] E. HaoYu, S. Cheng, K. Scott, B. Logan, *J. Power Sources* **2007**, *171*, 275–281.
[41] S. Cheng, H. Liu, B. E. Logan, *Environ. Sci. Technol.* **2006**, *40*, 364–369.

Manuscript received: March 11, 2017
Version of record online: May 23, 2017

